

Computational Analysis of Neutral Particle Fluxes from Non-Axisymmetric Magnetically Confined Plasmas

E.A. Veshchev¹, P.R. Goncharov², T. Ozaki², S. Sudo², J.F. Lyon³

1) Graduate University for Advanced Studies, Hayama, Kanagawa, 240-0193, Japan

2) National Institute for Fusion Science, Toki, Gifu 509-5292, Japan

3) Oak Ridge National Laboratory, Oak Ridge, TN 37831-8072, USA

Corresponding author's e-mail: veshchev.evgeny@lhd.nifs.ac.jp

Abstract

Energy and angle-resolved measurements of neutral particle fluxes from the plasma provide information about T_i , as well as non-maxwellian anisotropic ion distribution tails from NBI and ICH. Multidirectional diagnostics employing high resolution atomic energy spectrometers are being used to study the ion component heating mechanisms and fast ion confinement in helical plasmas. Since the natural atomic flux source is not localized in contrast to the diagnostic neutral beam or pellet charge exchange methods, the correct interpretation of such measurements in a complex toroidally asymmetric geometry requires a careful numerical modeling of the neutral flux formation and the knowledge of the charge exchange target distributions, relevant cross-sections and the magnetic surface structure. The measured neutral flux calculation scheme for LHD geometry is given. Calculation results for Maxwellian and NBI-induced ion distributions are shown. The behaviour of calculated and experimental suprathermal NBI tails is discussed along with the magnetic axis shift effect on energetic particle confinement.

1. Neutral Flux Formulation and Calculation Scheme

The atomic flux $\Gamma(E, \theta, t)$ [$\text{erg}^{-1}\text{s}^{-1}$] measured by passive diagnostics is an integral along the sightline \mathcal{L} of the local differential atomic birth rate in the plasma $g(E, \mathbf{r}, t)$ [$\text{erg}^{-1}\text{cm}^{-3}\text{s}^{-1}$], which contains the sought ion distribution:

$$\Gamma(E, \vartheta, t) = \frac{\Omega S_a}{4\pi} \int_{(\mathcal{L})} g(E, \vartheta, \mathbf{r}(\xi), t) e^{-\int_0^{\xi} \lambda_{mfp}^{-1}(E, \mathbf{r}(\xi'), t) d\xi'} d\xi, \quad (1)$$

where Ω is the observable solid angle and S_a is the diagnostic aperture area. The exponential factor describes the attenuation of the atomic flux in the plasma. $\lambda_{mfp}^{-1}(E, \mathbf{r}(\xi'), t)$ is the mean number of ionizations per unit path length. Changing the integration variable in (1) from ξ to the effective minor radius ρ yields [1, 2]

$$\Gamma(E, \vartheta, \zeta) = e^{\int_{\rho_{\min}}^1 Q^-(\tilde{\rho}, \zeta) \lambda_{mfp}^{-1}(E, \tilde{\rho}) d\tilde{\rho}} \frac{\Omega S_a}{4\pi} \int_{\rho_{\min}}^1 g(E, \vartheta, \rho) \times \left[Q^+(\rho, \zeta) e^{-\int_{\rho_{\min}}^{\rho} Q^+(\tilde{\rho}, \zeta) \lambda_{mfp}^{-1}(E, \tilde{\rho}) d\tilde{\rho}} - \right. \\ \left. - Q^-(\rho, \zeta) e^{-\int_{\rho_{\min}}^{\rho} Q^-(\tilde{\rho}, \zeta) \lambda_{mfp}^{-1}(E, \tilde{\rho}) d\tilde{\rho}} \right] d\rho. \quad (2)$$

The functions $Q^+(\rho, \zeta) = dX'/d\rho > 0$ and $Q^-(\rho, \zeta) = dX'/d\rho < 0$ on the intervals between $\rho = 1$ and $\rho = \rho_{\min}$ are obtained from the structure of the isolines $\rho = \text{const}$ known from a numerical solution of Grad-Shafranov equation [3]. This enables one to use the relation (2) for computer simulations of the neutral particle diagnostic data. Fig. 1 illustrates the calculation of the positive Q^+ and negative Q^- branches of the integral transform (2) for SDNPA

diagnostic [4]. The ion temperature retrieval from the thermalized spectra and modeling results for suprathermal high energy tails from NBI induced $f_i(E, \theta, t)$ are discussed below for LHD heliotron configuration.

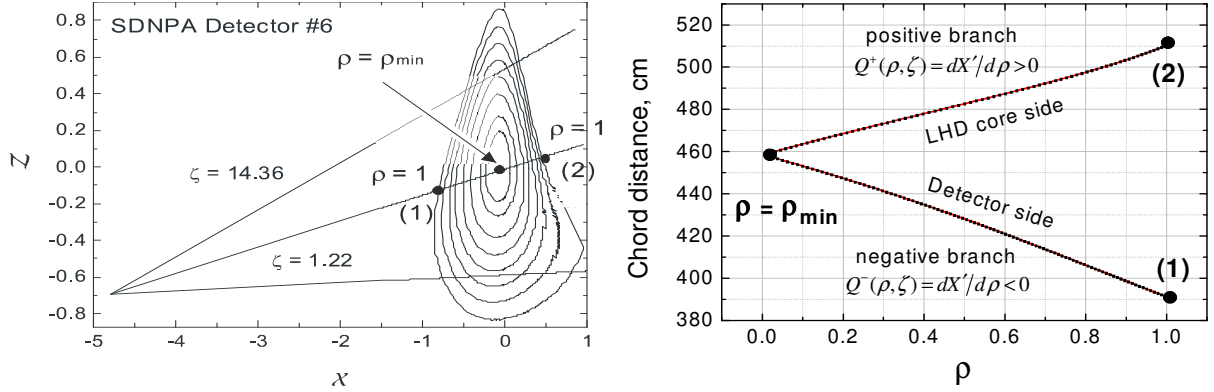


Fig. 1. Magnetic surface structure in SDNPA [4] detector #6 diagnostic cross-section (left) and the integral transform (2) kernel calculation for the middle vertical scan position (right).

2. Calculation Results for Maxwellian and Beam-induced Ion Distributions

The experimentally measured $\Gamma(E, \theta, t)$ has been calculated for hydrogen plasma on the following radial profile shape assumptions:

$$n_e(\rho) = n_e(0)(1 - \rho^a)^s, \quad T_e(\rho) = T_e(0)(1 - \rho^u)^w, \quad (3)$$

$$T_i(\rho) = T_i(0)(1 - \rho^x)^y, \quad (4)$$

$$n_0(\rho) = n_0(0) \exp(B\rho^A) \quad (5)$$

with the unknown values taken as free parameters. The hydrogen charge exchange $H^+ + H^0 \rightarrow H^0 + H^+$ and proton impact ionization $H^+ + H^0 \rightarrow H^+ + H^+ + e^-$ cross-sections were taken from [5].

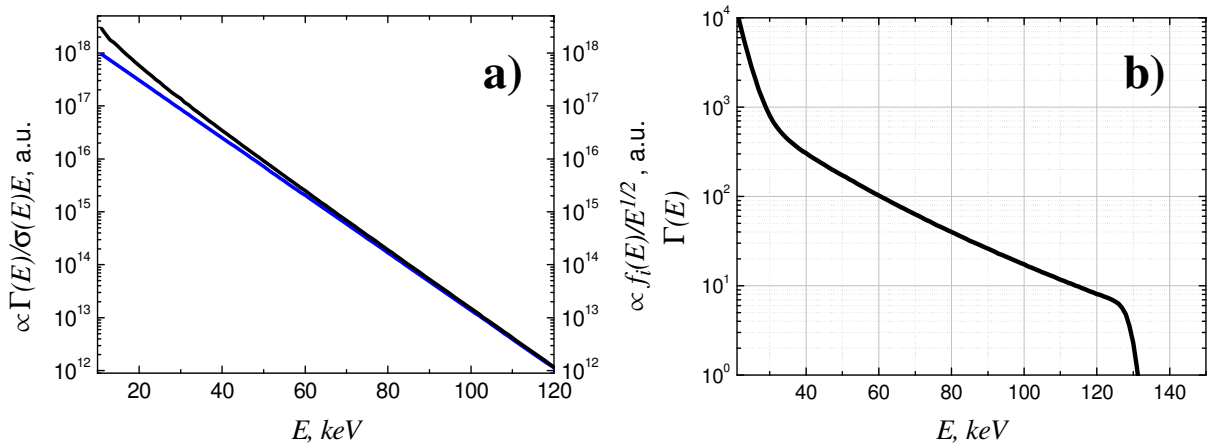


Fig. 2. a). Plasma with Maxwellian ion distribution: blue line – thermal $\exp(-E/T_i(0))$ representing the central ion temperature; black line – calculation of the experimentally measured neutral spectrum corrected for σE factor; b). NBI-heated plasma: calculation of the experimentally measured neutral spectrum.

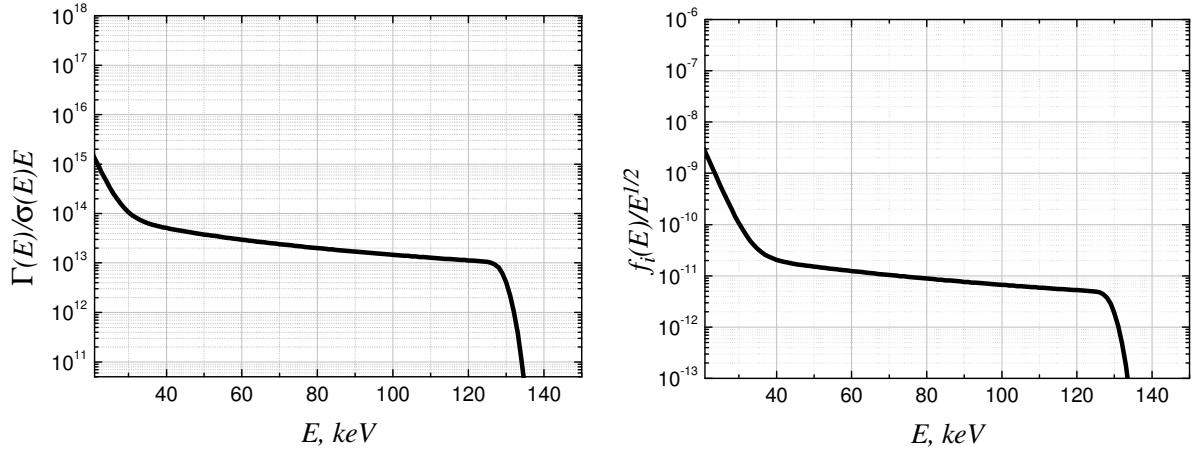


Fig. 3. NBI-heated plasma: calculated neutral spectrum corrected for σE factor (left); model ion distribution function (right)

Calculation results for the Maxwellian plasma ion distribution $f_i^{(M)}(E, \rho) = \frac{2\sqrt{E}}{\pi^{1/2} T_i^{3/2}(\rho)} \exp(-E/T_i(\rho))$ are shown in Fig. 2 a). The calculated typical neutral hydrogen energy spectrum corrected for the charge exchange reactivity factor $\sigma\sqrt{E}$ combined with the Jacobian \sqrt{E} (black line) and the Maxwellian exponent $\exp(-E/T_i(0))$ in the core region (blue line) are scaled to match at the highest energy in the considered range. Taking the logarithmic slope of $\Gamma(E)/\sigma(E)E$ in the energy range below $\approx 5T_i(0)$ as an estimation of the core T_i results in a systematic 10-30% error while at the higher energies this error vanishes. This is consistent with the simple qualitative analysis for a flat plasma layer case [6]. However, in practice either the counting statistics is poor at the highest energies or the high-energy tail becomes substantially non-Maxwellian due to the strong distortion by the ion heating.

In order to calculate the tangentially measured neutral hydrogen spectrum from tangential NBI heated Maxwellian background plasma, the model ion energy distribution was assumed to be a combination of the Maxwellian distribution function and the fast ion slowing down distribution from a monoenergetic isotropic source $S(v-v_0) = \frac{S_0}{4\pi v^2} \delta(v-v_0)$ [7, 8]:

$$f_i^{(s)}(v, t) = \frac{S_0}{4\pi} \frac{\tau_s}{v^3 + v_c^3} \left(h(v^*(v, t) - v_0) - h(v - v_0) \right), \quad (6)$$

where τ_s and v_c are the Spitzer's slowing down time and the critical velocity given by

$$\tau_s = \frac{3m_p T_e^{3/2}}{4\sqrt{2\pi} n_e e^4 \Lambda m_e^{1/2}}, \quad v_c^3 = \frac{3\sqrt{2\pi} T_e^{3/2}}{2m_p m_e^{1/2}}, \quad (7)$$

Λ is the Coulomb logarithm, $h(x)$ is the Heaviside step function and $v^*(v, t) = \left((v^3 + v_c^3) e^{3t/\tau_s} - v_c^3 \right)^{1/3}$.

Fig. 2 b) shows the resultant H^0 energy spectrum calculated in accordance with Eq. (2) with the integral kernel corresponding to detector #6 of the SDNPA diagnostic at the middle vertical scan position (see Fig. 1). The σE -corrected spectrum and the combined $f_i^{(M)}$ and $f_i^{(s)}$ ion distribution are shown in Fig. 3.

3. Analysis of Experimental Spectra from NBI-Heated Plasma

The calculation scheme described above taking into account the spectra superposition along the diagnostic chord and the isoline shape determined by the magnetic surface structure implies that a simple correction of the measured neutral spectra by the energy-dependent charge exchange reactivity factor $\sigma\sqrt{E}$ and the Jacobian \sqrt{E} may appear insufficient in case of complex-shaped full 3D plasmas. The correct interpretation of the neutral spectrum shape is important to draw conclusions on physical mechanisms responsible for the ion distribution formation.

Consider the experimental results illustrated by Fig. 4 representing the spectrum from SDNPA detector # 6 closest to the tangential observation direction measured from $n_e = 0.4 \times 10^{13} \text{ cm}^{-3}$ hydrogen target plasma at $R_{ax} = 3.6 \text{ m}$ heated by 130 keV H^0 NBI. The solid line shows the calculated neutral spectrum with free parameters chosen in such a way that the thermal slope and the value at the injection energy match the experimental ones (Fig. 4, left). The simple σE correction procedure leads to a U-shape tendency in the ion distribution (Fig. 4, right) with a decreased fast particle population. The calculation results suggest that this is an ion distribution property rather than a data misinterpretation. Fig. 5 shows the results for the similar plasma at $R_{ax} = 3.5 \text{ m}$.

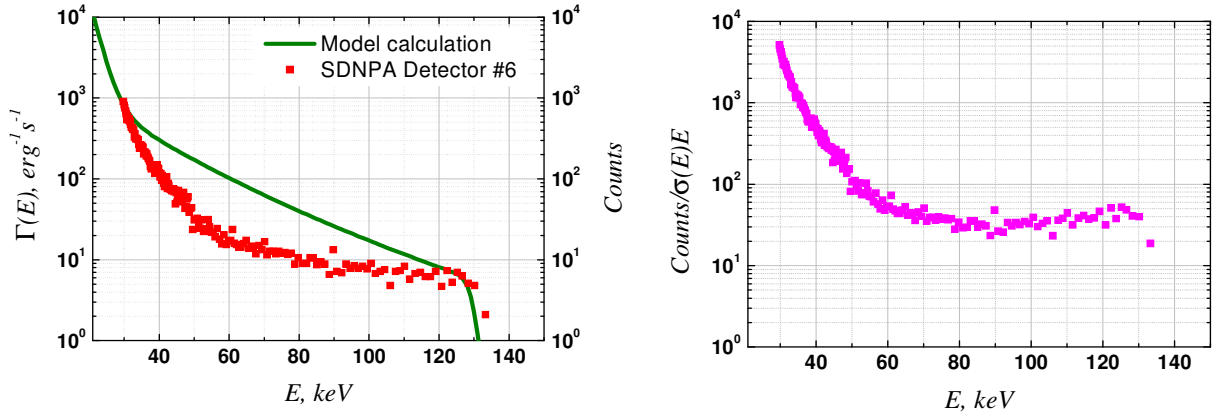


Fig. 4. $R_{ax} = 3.6 \text{ m}$; left: experimental (squares) and calculated (solid) neutral spectrum; right: σE corrected spectrum reflecting the ion distribution.

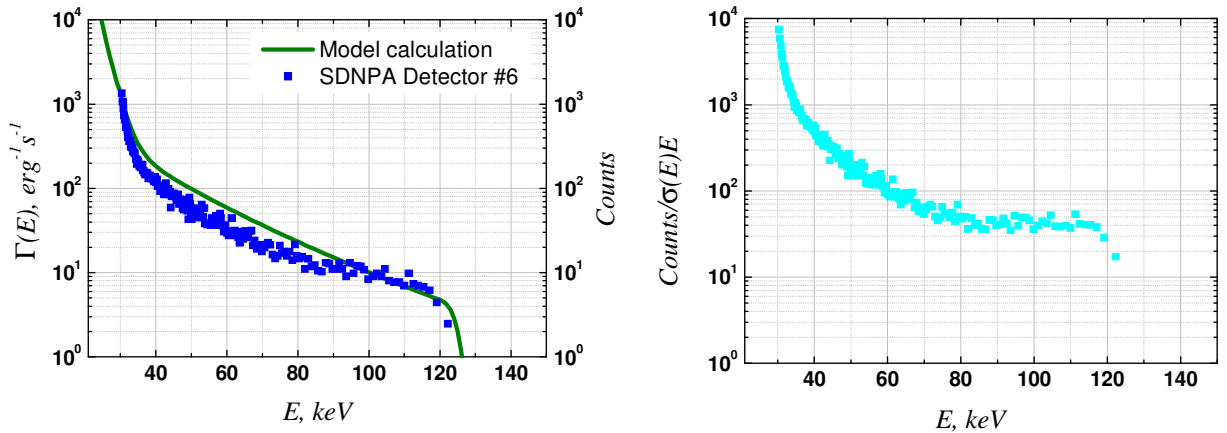


Fig. 5. $R_{ax} = 3.5 \text{ m}$; left: experimental (squares) and calculated (solid) neutral spectrum; right: σE corrected spectrum reflecting the ion distribution.

In order to validate the possibility of making comparisons between these spectra obtained at different R_{ax} positions, it is necessary to confirm that the geometry of measurements is not substantially different for these two cases. The magnetic axis shift leads to a certain displacement of the plasma column with respect to the diagnostic sightlines. The values of the effective minor radius and the pitch angle cosines of particles measured from different locations along the sightlines for $R_{ax} = 3.6$ m and for $R_{ax} = 3.5$ m were calculated. Since no enormous differences could be seen, it was accepted that for the two different magnetic configurations under investigation, the comparisons should be sensible between the spectra measured with the corresponding SDNPA detectors. Inward shifted plasmas exhibit an increased fast ion population. This is interpreted as a reduction of fast particle losses in comparison with the outward shifted case [9, 10].

4. Summary.

A scheme has been realized to calculate the energy resolved flux of neutral particles escaping from the helical plasma column. Thermal distributions have been analyzed for T_i determination. The presence of a systematic error in case of lower energy range usage has been demonstrated. Suprathermal distributions induced by tangential NBI have been analyzed to clarify kinetic effects and the effect of particle confinement on the distribution function. The effect of increased fast ion population in inward shifted R_{ax} configuration has been verified via the computational modeling of the escaping neutral fluxes and the experimentally obtained spectra analysis.

References

- [1] GONCHAROV, P.R., LYON, J.F., et al., *J. Plasma Fusion Res. Series*, **6** (2004), 314.
- [2] GONCHAROV, P.R., et al., *Proc. 31st EPS Conference on Plasma Physics and Controlled Fusion*, ECA vol. **28G**, P-5.112 (London, 2004).
- [3] LAO, L.L., HIRSHMAN, S.P., et al., *Phys. Fluids*, **24** (1981), 1431.
- [4] LYON J.F., GONCHAROV, P.R., et al., *Rev. Sci. Instrum.*, **74** (2003), 1873.
- [5] BARNETT, C.F., ed., *Atomic Data for Fusion*, ORNL-6086, USA (1990).
- [6] HUTCHINSON, I. H., *Principles of plasma diagnostics*, 2nd ed., Cambridge University Press, Cambridge (2002).
- [7] DNESTROVSKII, Y.N., KOSTOMAROV, D.P., *Numerical simulation of plasmas*, Springer-Verlag, Berlin (1986).
- [8] CORDEY, J.G., HOUGHTON, M.J., *Nucl. Fusion*, **13** (1973), 215.
- [9] LYON J.F., et al., *Proc. 29th EPS Conference on Plasma Physics and Controlled Fusion*, ECA vol. **26B**, P-1.102 (Montreux, 2002).
- [10] MURAKAMI, S., YAMADA H., et al., *Fusion Sci. and Technol.*, **46** (2004), 241.